J Mater Sci (2009) 44:2573–2580
DOI 10.1007/s10853-009-3336-8

Process parameters study on FSW joint of dissimilar metals for aluminum–steel

Thaiping Chen

Received: 7 November 2008 / Accepted: 10 February 2009 / Published online: 13 March 2009

Abstract This research aimed to weld dissimilar metals joints, AA6061 aluminum alloy and SS400 low-carbon steel, and find the optimum operating conditions of friction stir welding. In dissimilar metals butt joint by friction stir welding procedures, there are four major controllable factors, which are tool rotation speed, transverse speed (feed rate), tool tilt angle with respect to the workpiece surface and pin tool diameter. Understandably, not all the controllable factors are included in this article. The quality of dissimilar metals butt joints is evaluated by the impact value, which has not been discussed in literatures. In addition, an uncontrollable parameter, which is the tensile strength, is used to double-check its quality based on the excellent impact value. Analysis of variance (ANOVA) is used to analyze the experimental data. The Taguchi technique with ANOVA is also used to determine the significant factors of performance characteristics. The results are expected to serve as references to overland and aquatic transportation machines for weight reduction.

Introduction

Steel materials are inexpensive, its strength and toughness are extremely high and superior, and thus, steel has been the engineers' first choice of material. In general, the specific weight and stiffness of aluminum alloys used in the car industry are only about one-third of those of steel. Aluminum alloy has excellent specific weight properties; therefore, aluminum alloy is used extensively in air, overland, and aquatic transportation machines for their weight reduction capabilities. Furthermore, the steel materials welded to aluminum alloys that join technical parts are in great demand. For example, a vehicle's main structure, such as the steel-made chassis module, can be joined with secondary structural elements of aluminum alloy materials. Aquatic transportation vehicles prefer hulls made of steel and aluminum alloys; the under-water surface is made of steel, whereas, above the water surface, it is possible to use aluminum alloy. This structure not only lowers the center of gravity of the vehicles, but also achieves the reduction of their weight.

Friction Stir Welding (FSW) is a novel material-joining technique invented and patented [1] by The Welding Institute (TWI) in 1991, which can produce superior mechanical properties in the weld zone. The joining does not involve the use of any filler metals, and therefore, any aluminum alloy can be joined without concern for the compatibility of composition, which is an issue in fusion welding. In FSW processes, as presented by Chien et al. [1, 2], a non-consumable rotating tool with a specially designed pin and shoulder is inserted into the abutting edges of sheets or plates to be joined and traversed along the line of the joint. The heat is generated between the wear-resistant welding tool and the material of the workpieces. The heat causes the latter to soften without reaching the melting point and allows traveling of the tool along the welding line. Comparing the moving velocity of the tool and the heat traveling time of softening temperatures, the optimal tool moving velocity was determined by Chien et al. [3]. The method is solid state, and thus, is capable of joining dissimilar materials, as shown by [4] and [5], and at the same time avoiding many of the difficulties associated with fusion techniques. Recently, joining dissimilar materials by the FSW method has become a very hot issue. The

T. Chen (✉)
Department of Electrical Engineering, Fortune Institute of Technology, Kaohsiung 83160, Taiwan
e-mail: taiping@center.fotech.edu.tw

dissimilar materials can be dissimilar aluminum alloy [4, 5], or aluminum alloy to copper [6, 7], aluminum alloy to stainless steel [8–10], etc.

In the case of the FSW of aluminum alloy to stainless steel, Uzun et al. [8] studied the joints of AA6013-T4 aluminum alloy to X5CrNi18-10 stainless steel for their fatigue properties, hardness distributions, and classified seven different zones of the microstructure in the welding. The FSW joint of AA5083 aluminum alloy to SS400 low-carbon steel was investigated by Watanable et al. [9] for pin rotation speed effects on the tensile strength and the microstructure of the joint. The maximum tensile strength of the joint was about 86% of that of aluminum alloy-based metals. The FSW joint of AA6056 aluminum alloy to SS304 stainless steel was studied by Lee et al. [10] for its interfacial reaction, using transmission electron microscopy.

The purposes of this research are to weld dissimilar metals joints, namely, AA6061 aluminum alloy and SS400 low-carbon steel, and to determine the optimum operating conditions of FSW. The optimum operation is the combination of the four mainly controllable factors for the best quality of uncontrollable factors, such as impact value, and then verified by its ultimate tensile strength. The quality of FSW dissimilar metals butt joint evaluated by impact value has not been discussed in literatures, to the best knowledge of the author.

Experimental procedures

Experimental materials

This experiment uses the AA6061-T651 aluminum alloy plates, available in the market, with a thickness of 6 mm, and sections cut to a length of 160 mm by the width 40 mm. Aluminum alloy AA6061-T651 has an ultimate tensile strength with a maximum of 315 MPa. Low-carbon steel used are of Steel SS400 plates with a thickness of 6 mm, and an ultimate tensile strength of about 397 MPa. Two kinds of base metals, which are aluminum alloy AA6061-T651and steel SS400, are both milled to form smooth and flat surfaces for FSW processing specimens.

Friction stir welding (FSW)

This experiment, FSW, is performed on a vertical milling machine with a 5-Hp motor and a set of cone pulleys, with a total of eight speed changes of the belt transmission. The worktable has three axial operating directions. The X-axis direction may allow the auto-feed to move with a total of 12 speed changes. The gear reduction mechanism leads the screw transmission. Two milled specimens of the dissimilar metals are kept parallel adjoining each other and clamped on the worktable. The low-carbon steel is placed in the advancing side, as described [3]. The tool rotation is of clockwise direction. Tool tilt angle is tilting backward three degrees. In order to penetrate the low-carbon steel base metal about 0.1–0.2 mm, a suitable adjustment for the pin of the tool to be located on the side of the lower carbon steel is crucial. Before starting the welding process, the main axle begins rotation, and then the worktable is raised manually and slowly until the pin of the tool drills into the workpieces and the tool shoulder touches the workpiece surface. The worktable moves in the X-axis direction and the workpieces are welded. The workpieces clamped for the FSW processes and the FSW dissimilar metals joints are as shown in Fig. 1.

In this experiment, the material of the FSW tool is made of AISI 4140. The tool has a shoulder diameter of 20 mm, with the cylindrical pin having a diameter of 6 mm. In the FSW processing, the tool used is as shown in Fig. 2. In this study, four various parameters, as shown in Table 1, are performed on the milled specimens to weld dissimilar metals joints.

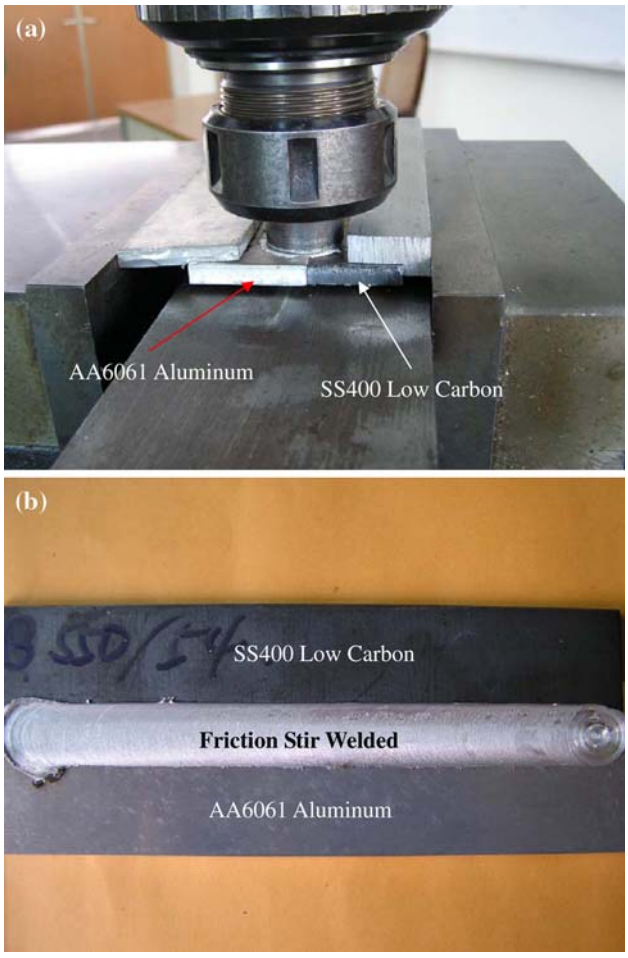

Fig. 1 Dissimilar friction stir welding for butt joints; **a** Dissimilar metals being welded and **b** Dissimilar metals joints with AA6061 aluminum alloy and SS400 low-carbon steel

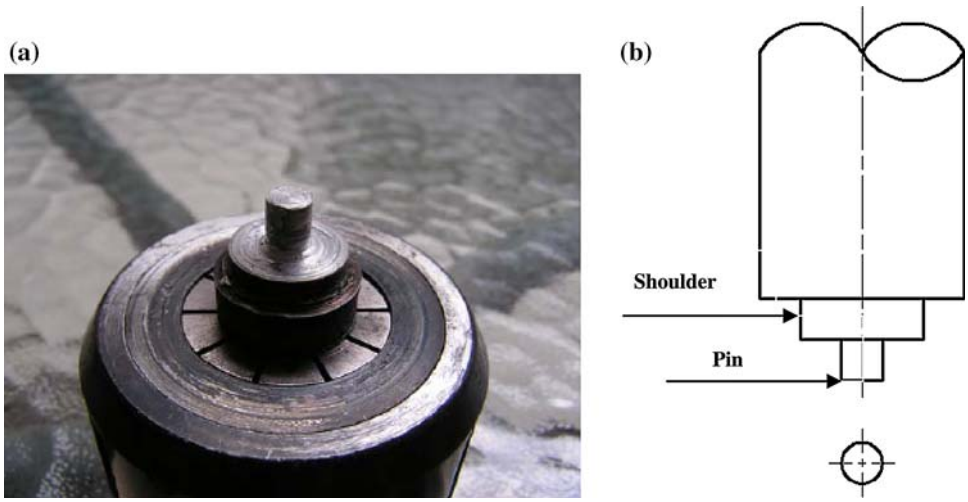

Fig. 2 The FSW tool used in this study; **a** Picture of tool and **b** Tool pin profile

Table 1 Process parameters and their levels

Process parameter	Unit	Level 1	Level 2	Level 3
Rotation speed; A	rpm	550	800	–
Transverse speed; B	mm/sec	0.9	1.2	1.5
Tool tilt angle; C	degree	1	2	3
Pin tool diameter; D	mm	6	7	8

Metallography and micro-Vicker's hardness test

The specimens for the micro-Vicker's hardness test are taken from the parts of the cross section, located at the welded zone of the FSW specimens, and along the vertical direction of the welding line. The specimens must be polished. Micro-Vicker's hardness data are taken at several locations at the top, middle, and bottom layers of the specimens. The spacing is 0.5 mm distance in each point. The loads of 300 g and 100 g are applied at the steel side and the aluminum alloy side, respectively. After observing the microstructure through the microscope at the nugget zone, the steel side is consumed by 5% Natal, and then the metallography is taken.

Tensile strength test

Each FSW specimen is cut to a 14-mm width, by a water-cooled grinding wheel, along the vertical direction of the welding pass. Then each specimen is milled to 12-mm width. Finally, the FSW-milled specimens are re-milled to form C-notch specimens for the ultimate tensile strength test, as shown in Fig. 3. The ultimate tensile strength test is performed on an Instron 8801 Universal Testing Machine. After the tensile strength testing, the fractured surfaces are scanned by Philies Quantum 200 scanning electron microscope (SEM).

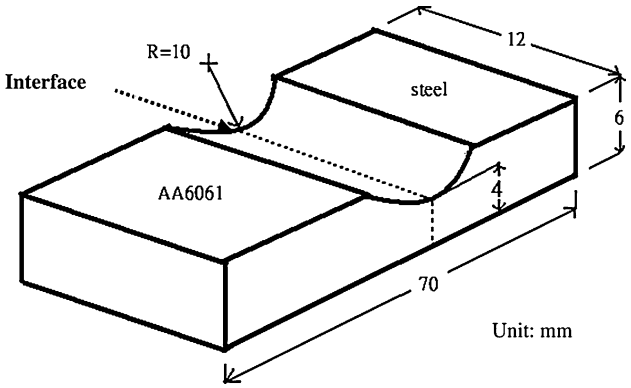

Fig. 3 C-notch tensile specimens dimension along the vertical direction of the welding line

Impact test

Similar to the method of manufacturing the C-notch tensile test specimens, each FSW specimen is cut to a 12-mm width, by a water-cooled grinding wheel, along the vertical direction of the welding pass. Then, the size of the each specimen is milled to a dimension of 55 mm × 10 mm × 6 mm. Finally, the FSW-milled specimens are re-milled to form C-notch specimens for impact testing, as shown in Fig. 4. The specifications of C-notch specimen geometry is adapted from the CNS 3033 U-notch geometry No. 3 Charpy specimen, as there are no prescribed specifications for dissimilar metals butt joints. The indentation is about 2 mm. The interface of low-carbon steel material and aluminum alloy deviates 3 mm from the centerline of the C-notch cavity. The impact values are performed on the Tinius Olson impact-testing machine under room temperature. Moreover, the resulting fractured mechanism is analyzed by SEM observation of the fractured surface.

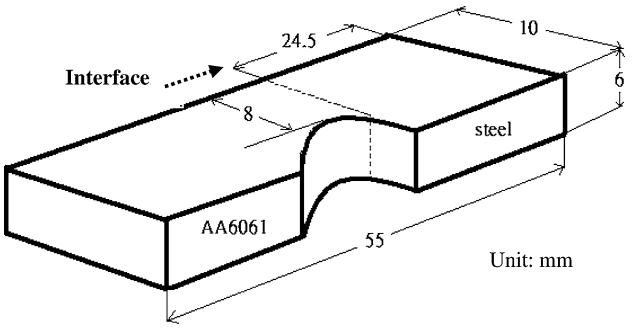

Fig. 4 C-notch impact specimens dimension along the vertical direction of the welding line

Analysis of variance (ANOVA)

ANOVA with the Taguchi technique is a statistic method used to interpret experimental data. In this study, there are four mainly controllable factors: two-level rotation speed (A; 550/800 rpm), three-level transverse speed (B; 0.9/1.2/1.5 mm/s), tool tilt angle (C; 1/2/3 degree), and pin tool diameter (D; 6/7/8 mm), as shown in Table 1, for analysis of variance. Their interactions are computed from the above experimental data for analysis of variance.

The desired characteristics of uncontrollable response factors can be measured by the impact values of the L_{18} (2×3^3), as shown in Table 2. Based on the use of Taguchi's recommendation [11], signal-to-noise ratio for impact value is:

$$\mathrm{SN} = -10\log_{10}\left(\frac{1}{m}\sum y^{-2}\right) \quad (1)$$

out of the m observations of y in each trial, the largest impact value is preferred. However, one of the uncontrollable parameters is the ultimate tensile strength, which is used to evaluate its quality, corresponding to excellent impact values. Therefore, in this article, the quality of dissimilar metals butt joints is evaluated by the impact value and ultimate tensile strength.

Results and discussions

Impact value

In this study, there are four mainly controllable factors, namely, the two-level rotation speed (A; 550/800 rpm), the three-level transverse speed (B; 0.9/1.2/1.5 mm/s), the tool tilt angle (C; 1/2/3 degree), and the tool pin diameter (D; 6/7/8 mm), as shown in Table 1, for analysis of variance. The desired characteristic of uncontrollable factors for the response was measured by C-notch Charpy impact values, as shown in Table 2. Based on the use of the impact values, the larger the value the better it is.

Table 2 The FSW process data of L_{18} orthogonal arrays

Trial no.	Process parameter levels				Impact values (J)		
	A	B	C	D	No. 1	No. 2	No. 3
1	1	1	1	1	36.1320	36.1320	35.6145
2	1	1	2	2	43.2119	46.4119	48.2929
3	1	1	3	3	49.3723	50.9976	41.3601
4	1	2	1	1	18.6475	21.5480	10.2091
5	1	2	2	2	15.5539	23.0140	22.2797
6	1	2	3	3	10.4380	16.2633	19.8509
7	1	3	1	2	20.0925	20.3343	22.0355
8	1	3	2	3	18.6475	31.0021	34.0679
9	1	3	3	1	11.1266	10.2091	9.9806
10	2	1	1	3	5.2571	4.3742	4.8150
11	2	1	2	1	22.0355	22.5242	23.5050
12	2	1	3	2	24.9846	24.4903	25.2322
13	2	2	1	2	35.3561	38.2118	35.0980
14	2	2	2	3	3.9348	4.1543	3.4968
15	2	2	3	1	11.5872	8.1639	8.3898
16	2	3	1	3	33.5544	31.7651	36.1320
17	2	3	2	1	7.4881	7.0392	7.0392
18	2	3	3	2	1.9746	3.2783	3.2783

Table 3 ANOVA summaries of the impact values

Source	Sum of squares	Degree of freedom	Mean sum of squares	F-ratio
A	1511.2	1	1511.2	11.76[a]
B	2082.7	2	1041.4	8.11[a]
C	363.8	2	181.9	1.42
D	603.9	2	301.9	2.35
Error	5909.5	46	128.5	
Total	10471.1	53		

[a] At least 95% confidence

The ANOVA summary results of the C-notch Charpy impact values are as shown in Table 3. The results correspond to at least 95% confidence, which indicate that rotation speed and transverse speed are relatively the significant FSW process parameters, respectively. The significant factors can be identified from the values of their F ratios. The tool tilt angle and pin diameter are not relatively significant FSW process parameters for the C-notch Charpy impact values.

The most effective FSW process parameter for the C-notch Charpy impact values, as shown in Table 4, is the transverse speed. In Table 4 and Fig. 5, the optimal FSW process parameters for impact quality are shown as derived from a combination of rotation speed of 550 rpm, transverse speed 0.9 mm/s, tool tilt angle one degree, and tool pin diameter 7 mm. The effects of the control factors are in order of transverse speed, rotation speed, tool pin diameter,

Table 4 Response table for the impact values

Levels	Factors			
	A	B	C	D
1	26.8	30.3	24.7	17.1
2	16.2	17.0	21.3	25.2
3	–	17.2	18.4	22.2
Max–min	10.6	13.3	6.3	8.1
Rank	2	1	4	3

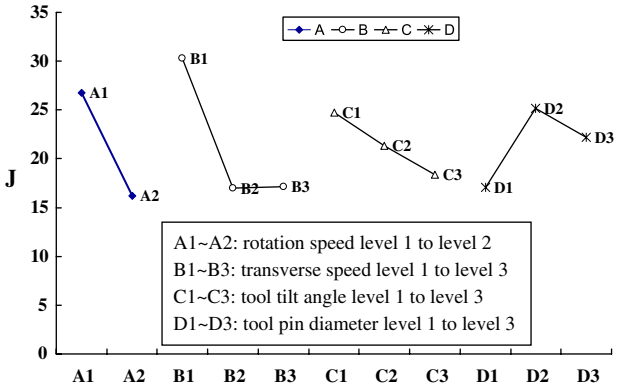

Fig. 5 The effect of controllable parameters for the C-notch impact value (J)

and tool tilt angle. The rotation speed of 800 rpm gives the worst C-notch Charpy impact value. The transverse speed 0.9 mm/s gives the best C-notch Charpy impact value. The lower transverse speed and rotation speed will give the higher C-notch Charpy impact value; however, it requires more information for further confirmation. As transverse speed increases, the impact value decreases, although impact values showed little difference in the speeds ranging between 1.2 and 1.5 mm/s. Tool tilt angle is inversely proportional to the impact value. Pin tool diameter is a non-linear effect. The quality of FSW dissimilar metals butt joints evaluated by impact value has not appeared in previous literatures, to the best knowledge of this author. Therefore, there is no comparison of the impact values with results of literatures.

In Fig. 5, the vertical axis (Coordinate) represents the response of the uncontrollable parameter, such as impact value in Joule. The transverse axis (Coordinate) represents the levels of the controllable parameters— the four major controllable factors are: the two-level rotation speed (A; 550/800 rpm), the three-level transverse speed (B; 0.9/1.2/1.5 mm/s), the tool tilt angle (C; 1/2/3 degree), and the tool pin diameter (D; 6/7/8 mm). The symbols A1 and A2 represent rotation speed level 1 and level 2, respectively. B1, B2, and B3 are the transverse speed level 1, level 2, and level 3, respectively. C1, C2, and C3 are the tool tilt angle level 1, level 2, and level 3, respectively. D1, D2, and D3 are the tool pin diameter level 1, level 2, and level 3, respectively.

The specimens bending formations after the C-notch Charpy impact tests are as shown in Fig. 6. The results indicate that the specimens of the rotational speed 550 rpm, combined with three different transverse speeds, have obvious plastic deformation before breaking. The transverse speed of 0.9 mm/s gives the best quality. The specimen is bent to 150-degree angle, and remains not broken apart, as shown in Fig. 6a. In addition, both the base materials for the C-notch specimen impact test are bent but not broken apart. In the case of rotational speed of 800 rpm, the impact value is almost zero and the specimen is brittle and broken along the interface, as shown in Fig. 6b, for all of the transverse speeds. The smooth cleavage surfaces are brittle fractured. The parallel strips must be the scratch traced by the tool pin in low-carbon steel. In the tough breaking area, many fragments of the steel were scattered in the aluminum alloy matrix, as shown in Fig. 7a. The magnified picture in the tough breaking area, as shown in Fig. 7b, reveals a coral reef-like structure.

The bright area is composed of steel fragments and is located at the welding zone center. The cleavage lines tend to occur along the interface between the fragment and the aluminum matrix. To reduce the production of the cleavage lines, which may be micro-cracks or intermetallic compounds, is to conduct toward favor enhances their joints toughness. In this experiment, the small frictional thermal

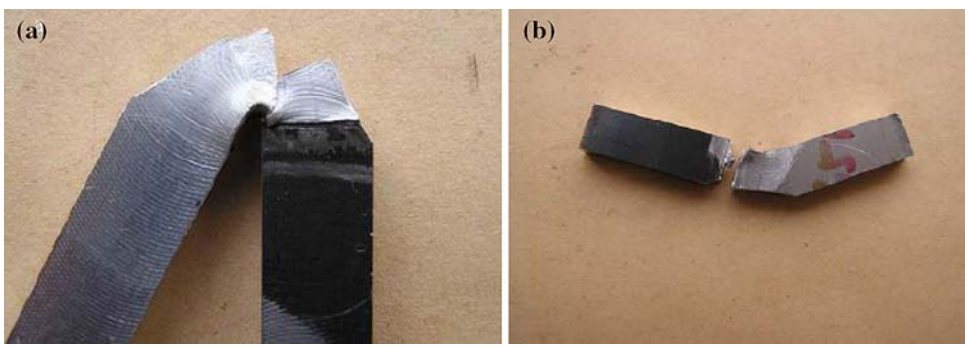

Fig. 6 Specimen bending situations after impact tests; **a** Ductile bending and not broken apart and **b** Brittle and broken apart along the interface

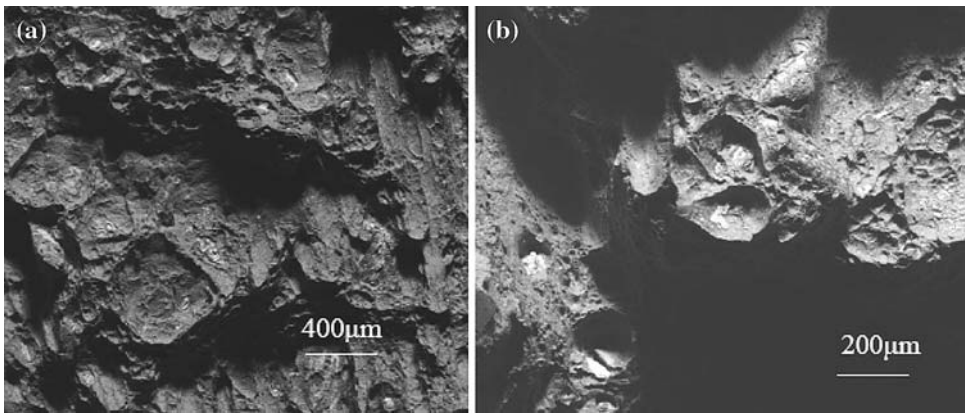

Fig. 7 Electron microscope pictures in the breaking area in the impact FSW specimens; **a** Macroscopic view and **b** Partially enlarged pictures

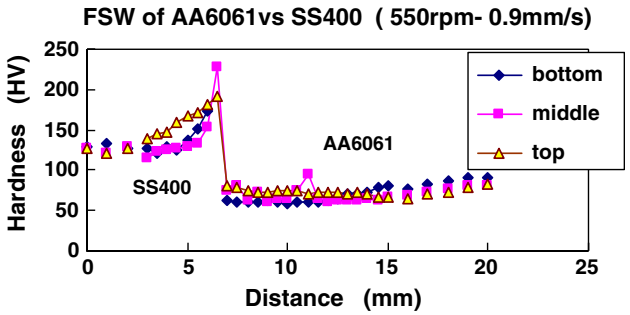

Fig. 8 Hardness distribution in the FSW joints of the aluminum alloy and the low-carbon steel

energy produced by the low rotational speed is difficult to generate at the cleavage line. More details are referred to in the next section.

Hardness distribution and metallography

As noted in section "Impact value", the optimal FSW process parameters for the impact quality is derived from a combination of the rotation speed of 550 rpm and the transverse speed of 0.9 mm/s. The hardness distributions in the optimal FSW joint of aluminum alloy and low-carbon steel are shown in Fig. 8. The hardness in low-carbon steel base metal is about Hv 120. In the near interface, 1.5 mm the hardness elevates gradually to about Hv 225. The phenomenon indicates work hardening during FSW tool stirring. The nugget zone area is about 6 mm in width, and the hardness changes to become quite large in the greatest hardness zone. This is because of the test points being located at the large fragments of the steel material, as shown in Fig. 9. The small fragments of the steel material spread throughout the entire FSW zone, and their hardness fell to about Hv 50–80.

In the FSW joints of aluminum alloy and low-carbon steel, the nearby interface metallography in the welding area demonstrates the steel fragments with non-uniform distribution. The various sizes of the steel fragments

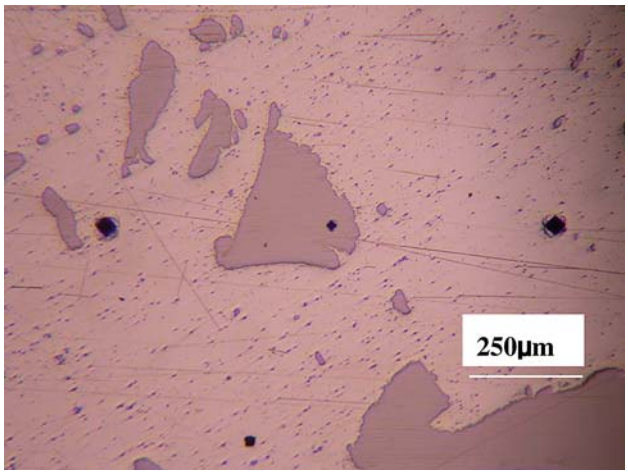

Fig. 9 Various sizes of the steel fragment dispersions in the entire nugget zone

resemble to the onion shapes in the metallography, as shown in Fig. 10a. The thermal-mechanically affected zone (TMAZ) and heat-affected zone (HAZ) in the SS400 side are difficult to observe. The HAZ in the AA6061 side is out of the Fig. 10a. Although their interfaces in the enlarged picture, as shown in Fig. 10b, have obviously inequalities, it is extreme butt-welded. In the nugget, the steel fragments are surrounded by a gray outer covering (GOC), as shown in Fig. 10c, and some cracks can be clearly observed within the GOC, in the thick and dense positions. The specimens after applied impact tests are brittle, which could be verified from GOC of the SEM images. In Fig. 10b, GOC is not found at the interface between AA6061 and SS400. The brittle specimens with low impact values have SEM images similar to Fig. 10c, and the tough specimens with high impact values are similar to Fig. 10b.

Tensile strength

Based on the ANOVA summary results of the C-notch Charpy impact values, the tool tilt angle and pin diameter

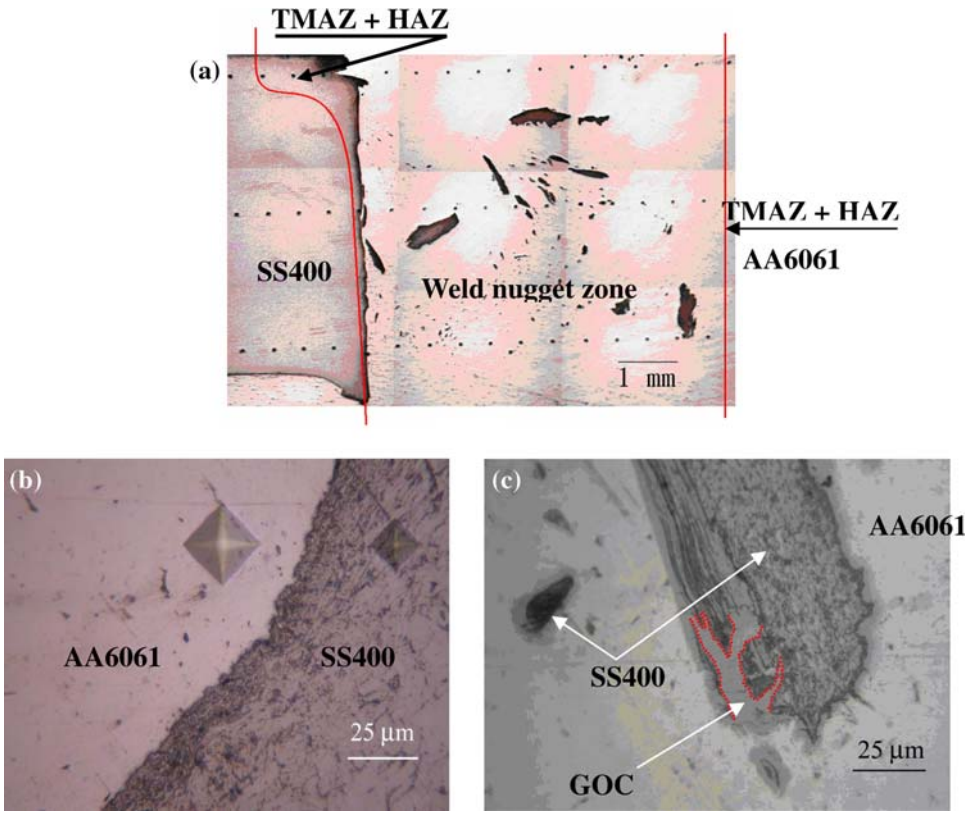

Fig. 10 Welded zone metallography in the FSW joints; **a** Macroscopic metallography, **b** Microscopic metallography, and **c** Steel fragments surrounded by a gray outer covering (GOC)

are not relatively significant FSW process parameters. Then, tool pin diameter of 6 mm and tool tilt angle of three degrees are adapted for the tensile test specimens in the FSW process. The rotation speed of 800 rpm gives the worst C-notch Charpy impact value. For the tensile test, the controllable factors have narrowed down to rotation speed (550 rpm) and transverse speed (0.9/1.2/1.5 mm/s). The results of the tensile strength are shown in Table 5. The best transverse speed is 1.2 mm/s, with tensile strength of 240 MPa. The transverse speeds 0.9 mm/s and 1.5 mm/s yielded the values of 225 and 233 Mpa, respectively. AA6061 base material has the ultimate tensile strength of about 315 MPa. The maximum tensile strength of the dissimilar joint is about 76% of the AA6061 base material. The maximum tensile strength of the FSW dissimilar joints in literature [9] is about 86% of the Al base material, although it is a different base material, namely, AA5083. The optimal FSW process parameters for impact quality are the combination of the rotation speed of 550 rpm and the transverse of speed 0.9 mm/s, which are acceptable in the FSW processes for tensile strength.

Table 5 Tensile strength (MPa)

Transverse speed	Rotation speed	
	550 rpm	800 rpm
0.9 mm/s	225	160
1.2 mm/s	240	233
1.5 mm/s	233	234

The C-notch specimens of the tensile test broke from the nearby interface of aluminum alloy and low-carbon steel. However, in the well down FSW joints, the breaking lines are moving at 15–30 degree angles with the interface to the aluminum alloy side. This may imply massive plastic deformations before the specimens broke, as shown in Fig. 11. The fractured surface observation used an electron microscope, with secondary and reflection electron-mixed image formation functions. In Fig. 12, the bright area is the steel. In the upper half of the picture, the white areas show the cleavage

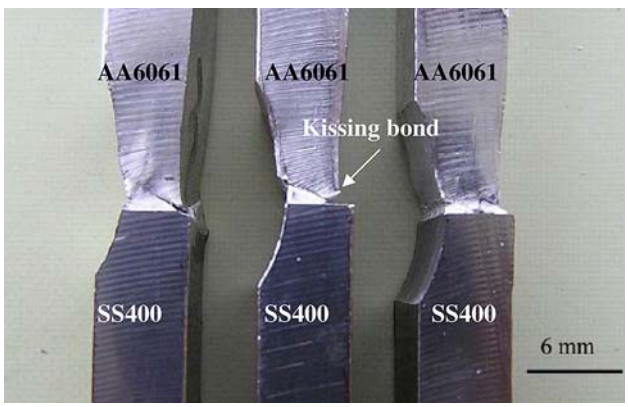

Fig. 11 Specimens after tensile tests, broken from the nearby adjoining plane of the aluminum alloy and the low-carbon steel

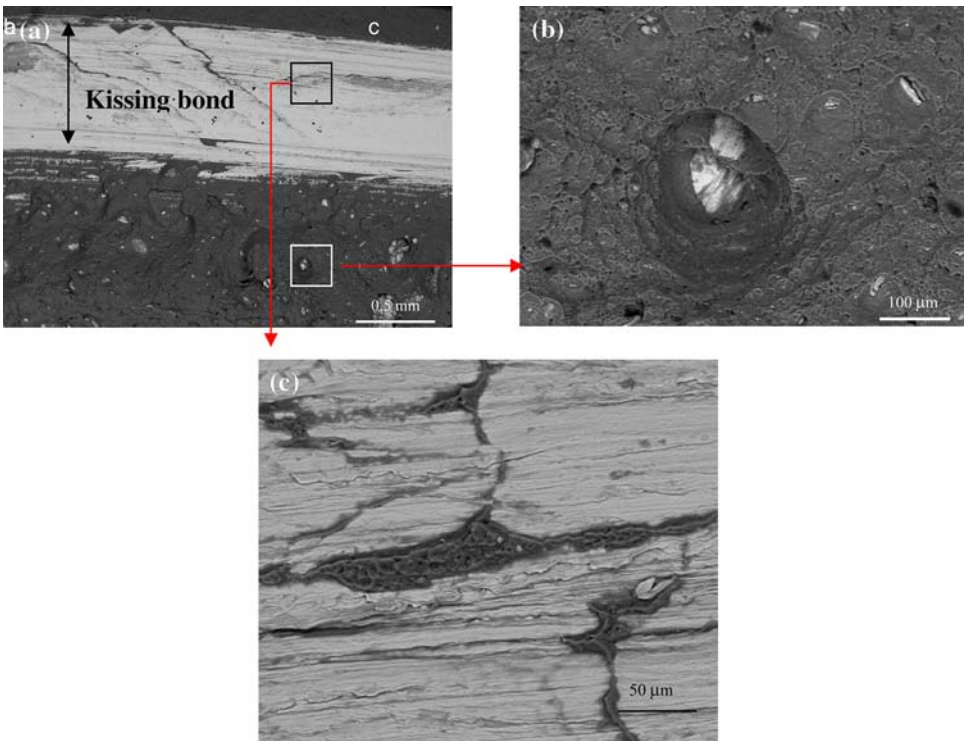

Fig. 12 Electron microscope pictures for the breaking surface in the tensile specimens of the steel and aluminum alloy joints; **a** macroscopic view, **b** and **c** partially enlarged pictures

surface along the interface of the aluminum–steel. In the lower part of the picture, dark areas show an irregular rough surface with some of the aluminum alloy sticking in the lower carbon steel side. The white spots show the steel fragments in the nugget. Characteristic ductility is shown in Fig. 12a. In the enlarged picture, as seen in Fig. 12b an obvious concave dimple appears, which identifies the concave nest shape as a low-carbon steel fragment.

Conclusions

The dissimilar metals butt joints for AA6061 aluminum alloy and SS400 low-carbon steel materials have been successfully produced by the method of friction stir welding. The lower transverse speed and rotation speed, which are the significant FSW process parameters, yield a higher C-notch Charpy impact value. The transverse speed of 0.9 mm/s, combined with a rotation speed of 550 rpm yields the best quality of impact values, and an acceptable quality of tensile strength. This best quality specimen can be bent to 150 degree angle and remain not broken apart.

Acknowledgements The author gratefully acknowledges the financial support received from the National Science Council (grant no. 96-2221-E-268-003), and the National Center for High Performance Computing of the Republic of China.

References

1. Thomas WM (1995) GB Patent Application 91259788 (1991). US Patent 5460317
2. Chien CH, Chen TP, Chao YJ (2005) J CSME 26:195
3. Chien CH, Chen TP, Lin WB, Chao YJ (2006) J CSME 27:663
4. Steuwer A, Peel MJ, Withers PJ (2006) Mater Sci Eng A 441:187
5. Karlsson L, Berqvist EL, Larsson H (2002) Weld World 46:10
6. Lee WB, Jung SB (2004) Mater Res Innov 8:93
7. Ouyang J, Yarrapreddy E, Kovacevic R (2006) J Mater Process Technol 172:110
8. Uzun H, Dalle Donne C, Argagnotto A, Ghidini T, Gambaro C (2005) Mater Design 26:41
9. Watanable T, Takayama H (2006) J Mater Process Technol 178:342
10. Lee WB, Schmuecker M, Mercardo UA, Biallas G, Jung SB (2006) Scr Mater 55:355
11. Ross PJ (1996) Taguchi techniques for quality engineering. McGraw-Hill, New York